Performance Evaluation of Digital Modulation Techniques Used in Bluetooth Physical/Radio Layer

Islam Galal[1], Mostafa E. A. Ibrahim[1], Hossam E. Ahmed[1]
and Abdelhalim Zekry[2]
[1]Electrical Engineering Department- Benha Faculty of Engineering - Benha University
[2]Electronics And Communications Department - Faculty of Engineering - Ain Shams University
Email: {islam.galal, mustafa.ibrahim and hossameldin.ibrahim}@bhit.bu.edu.eg and aaazekry@hotmail.com

***Abstract*— Most Bluetooth implementations focus on architecture, routing protocols, encryption, and performance evaluation of the network. This paper provides a brief description of the Bluetooth standard including the physical layer. It focuses on developing MatLab/Simulink models for the Bluetooth transceivers utilizing different modulation schemes and the performance evaluation of these models. Different pulse shaping waveforms are utilized in our Matlab/Simulink Bluetooth models. The performance of our Bluetooth transceiver models with AWGN channel is evaluated by means of the BER.**

I. Introduction

Recently, the increasing demand for wireless communication systems has elevated the employment of advanced modulation schemes to explore their advantages and performance. The leading concerns of modern digital modulation techniques are to achieve modulation with power spectrum of acceptable bandwidth, to generate a modulated signal with constant amplitude and to attain minimum Bit Error Rates (BER) [1], [2], [3], [4].

In this paper, we consider the Bluetooth as an example of wireless communication systems. Our focus goes to the Bluetooth physical layer which concerns the modulation issue. Consequently, we examine several advanced modulation schemes namely: Gaussian Frequency Shift Keying (GFSK), $\pi/4$ shifted Differential Quadrature Phase Shift Keying ($\pi/4$ DQPSK) , and $\pi/8$ shifted Differential Eight Phase Shift Keying ($\pi/8$ D8PSK) from the perspectives of BER, spectral efficiency, and hardware complexity. In addition, the physical layer model developed in this paper is a basic step in Software Defined Radio (SDR) implementation of the bluetooth transceiver.

The rest of the paper is organized as follows: Section II describes prior research efforts related to this work. Section III gives an overview of the Bluetooth physical layer and the Bluetooth transceiver specifications. Section IV describes in detail the utilized modulation techniques by mathematical analysis. Section V illustrates the achieved transmission performance of applying different digital modulation techniques. Moreover, transmission performance of each modulation scheme is evaluated and compared with the aid of the statistical distribution and BER evaluation. Finally, Section VI summarizes the main contributions of this paper.

II. Related Work

In this paper we focus on the Bluetooth physical layer implementation. However, topics such as advanced modulation schemes, Adaptive Frequency Hopping (AFH), and data rates are closely related to the Bluetooth physical layer. Therefore, in this section we review the evolution and state-of-the-art in the aforementioned topics.

Choi et al. [5] proposed six hardware and software schemes for area reduction and simple implementation, They designed a Bluetooth Enhanced Data Rate (EDR) baseband controller using unified GFSK, $\pi/4$ DQPSK, and D8PSK. The FPGA implementation was shown to be fully matched with enhanced data rates of $2Mbps$ and $3Mbps$. But their results show no BER for the implemented systems. Shuaib et al. [6] developed several MATLAB/Simulink simulations to evaluate the performance of Zigbee/IEEE $802.15.4$ physical layer. The simulation results show how the BER versus the SNR values were affected when varying communication parameters such as the input data rate, the level of the AWGN power and number of bits per symbol.

Spill et al. [7] presented techniques for eaves dropping on Bluetooth data. They showed how packets can be intercepted, un-whitened, and how to decrypt data in the case of encryption. They obtained the necessary parameters for calculating the hopping sequence. But, they only studied the GFSK modulation scheme and without studying other security modes used in Bluetooth v2.0. Binh et al. [8] investigated the use of linear and nonlinear phase shaping filtering and their impacts on Minimum Shift Keying (MSK) modulated optical signals transmission over optically amplified long haul communications system. Transmission performance obtained indicates the resilience of the MSK signals in transmission over multi-optically amplified multi-spans. But, they only studied the impact of one pulse shaping on the channel.

Kanna et al. [9] designed MSK modulation technique by using MATLAB/SIMULINK and showed that the theoretical maximum bandwidth efficiency of MSK is $2bits/s/Hz$ which is the same as for QPSK and Offset QPSK (OQPSK) and confirmed the viability of theoretical approach. They employed Zigbee technology by OQPSK modulation with half sine pulse shaping. Morsi et al. [10] examined, estimated and evaluated the performance of Frequency Hopping (FH) selection kernel,

978-1-4673-2961-3/12/$31.00 ©2012 IEEE

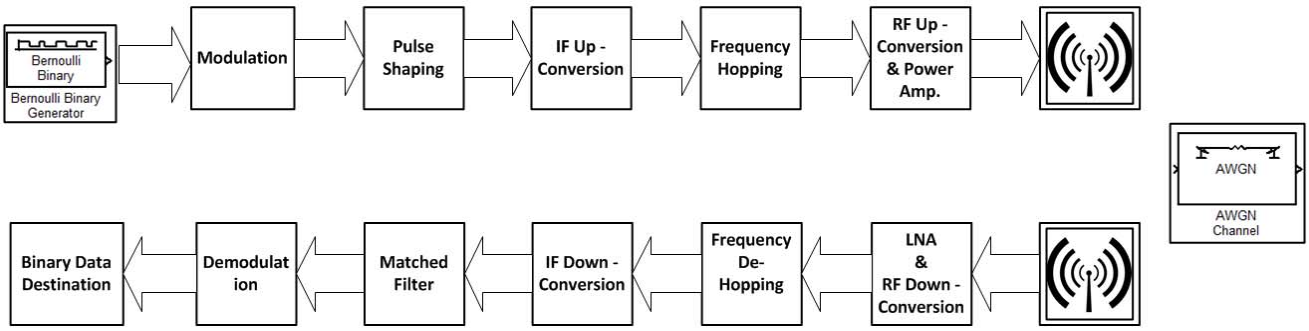

Fig. 1. General Block Diagram of a Typical Bluetooth Physical Layer Transceiver.

used in the Bluetooth to implement FH technique, verified by theoretical analysis and simulation results that compared to purely random hopping sequences the Bluetooth hopping sequence offers noticeable residual correlations and periodic cross-correlations features. But, their results didn't illustrate the effect of various modulation methods impact on the FH. Schiphorst et al. [11] discussed several demodulation algorithms for Bluetooth GFSK signals. In order to evaluate the performance of the algorithms, they built a Bluetooth simulation model. In this model, Bluetooth packets were generated, transmitted and demodulated by different demodulation algorithms. They tried to combine two different types of standards, Bluetooth and HiperLAN/2 on one common hardware platform.

III. Bluetooth Physical/Radio Layer

As with any other wireless communication technology, the main functions of the physical layer are spreading, despreading, modulation and demodulation of the signal. At the physical layer, Bluetooth operates in the ISM band at $2.4GHz$ with a bandwidth of about $80MHz$ depending on the country.

What makes bluetooth different from other wireless communication technologies that it divides the ISM band into 79 channels and employs frequency hopping technique with a fast hop rate of $1.6Khps$ to combat interference and fading. In order to derive a hopping sequence, we utilize a pseudo random number generator that applies Linear feedback shift register instead of using master clock and $48-bit$ PIN address. Hence, in our developed Bluetooth transceiver models shown in Fig.(1) the hopping rate is changed to $160Khps$ instead of $1.6Khps$ to clearly illustrate the hopping sequence in the simulation results.

A Gaussian shaped binary FM modulation (GFSK) is applied to minimize the Bluetooth transceiver complexity. For EDR, two variants of the PSK modulation schemes namely: $\pi/4$ DQPSK and $\pi/8$ D8PSK are utilized. The symbol rate for all modulation schemes is $1Ms/s$. The gross air data rates are $1Mbps$, $2Mbps$ and $3Mbps$ for GFSK, $\pi/4$ DQPSK and $\pi/8$ D8PSK respectively. A slotted channel is applied with a nominal slot length of 625μSec. For full duplex transmission, a Time-Division Duplex (TDD) scheme is utilized [12].

Bluetooth hopping pattern algorithm is implemented by giving a window of 32 frequencies in the $2.402GHz$ to $2.483GHz$ range. These frequencies are randomly chosen. Once all the 32 frequencies in that set have been visited once, a new window of 32 frequencies is selected. This new window includes 16 of the frequencies previously visited and 16 new frequencies [13].

IV. Methodology

In this section, we illustrate our methodology to evaluate the performance of advanced modulation schemes applied in a Bluetooth transceiver. First, we present an overview of the GFSK modulation scheme. Then, we explain the $\pi/4$ DQPSK modulation scheme. Finally, we illustrate the $\pi/8$ D8PSK modulation scheme. The pre-mentioned three modulation techniques are evaluated using Matlab/Simulink ver. $R2011b$ (7.13.0.564).

A. GFSK Modulation

GFSK is a kind of Continuous Phase Frequency Shift Keying (CPFSK) modulation technique originated from FSK which is a well known power efficient modulation scheme with a constant envelope. Since the modulated signal has constant amplitude (constant envelop), an efficient RF amplifier of class C can be used to minimize power consumption, an important consideration for battery-powered units. However, the bandwidth requirement of FSK significantly increases as the number of modulating symbols increases. Therefore, in modern Bluetooth low data-rate applications, GFSK modulation employs the Gaussian function as a pulse shaping filter to reduce transmission bandwidth.

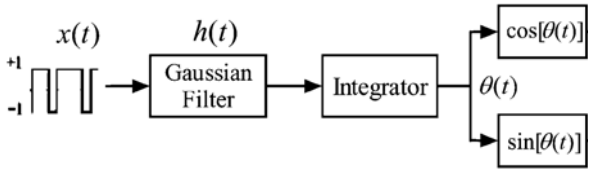

Fig. 2. GFSK Modulator.

Figure(2) illustrates the GFSK modulation wherein the input data rate of $1Mbps$, which is represented by its equivalent Non-Return to Zero (NRZ) data stream: $x(t)$, is applied to the Gaussian filter: $h(t)$. This filter is characterized with a Bandwidth Time product $BT = 0.5$. The output of the Gaussian filter is then applied to an integrator which converts the amplitude levels to phase changes. Then, it applied to a Quadrature Frequency Synthesizer which generates the In-phase and Quadrature complex baseband signals (I, Q). In order to exploit the maximum available channel bandwidth, the gain of the integrator varies the modulation index β in the range $0.28 - 0.35$ [14].

The (I, Q) signals are then up-converted to the IF frequency band as indicated in Eq.(1) and Eq.(2). Thus, to convert it to the constant envelop representation we represent the signals in complex envelop representation and select positive pre-envelop. The output of the GFSK modulator is applied to the AFH sub system followed by the RF frequency up-conversion.

$$s_{GFSK}(t) = \sqrt{\frac{2E_b}{T_b}} \left[\cos\varphi(t,\alpha)\ \cos 2\pi f_c t\ \right] - \left[\sin\varphi(t,\alpha)\ \sin 2\pi f_c t\ \right] \quad (1)$$

Equation(2) gives the phase modulation (φ) process where (α_i) is the NRZ binary data sequence.

$$\varphi(t,\alpha) = \frac{\pi}{2T_b}\sum_i \alpha_i \int \left[Q\left(\frac{2\pi BT_b}{\sqrt{\ln 2}}\left(\frac{\tau}{T_b} - (i+1)\right)\right)\right] - \left[Q\left(\frac{2\pi BT_b}{\sqrt{\ln 2}}\left(\frac{\tau}{T_b} - i\right)\right)\right] d\tau \quad (2)$$

In the receiver path, we use differential decoding scheme by Least Squares/Maximum Likelihood methods to demodulate the received GFSK signals utilizing the discrete time quadricorrelator as shown in Fig.(3) [15].

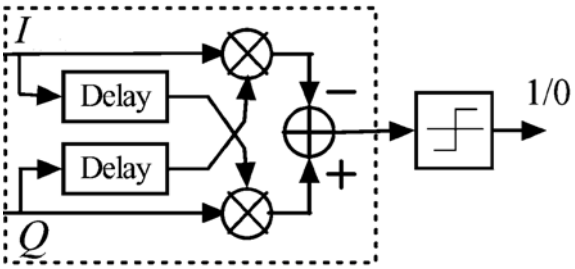

Fig. 3. GFSK Demodulator Utilizing Discrete Time Quadricorrelator.

B. $\pi/4$ DQPSK Modulation

PSK systems represent the transmitted data signal by varying the phase of a fixed frequency carrier. DPSK is a special scheme of PSK modulation techniques which is significantly reduce the hardware complexity. Since the DPSK is a non coherent scheme, it does not require carrier recovery circuit. DPSK also reduces the adversary effect of the fading channel.

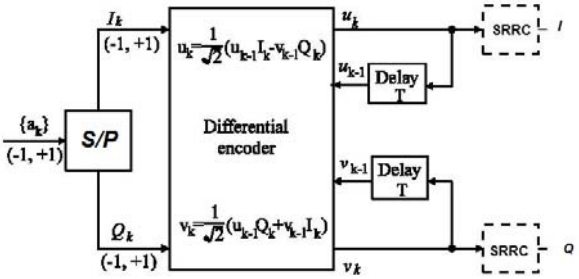

Fig. 4. $\pi/4$ DQPSK Modulator.

In the other hand , it produces more erroneous demodulations.

Figure(4) illustrates the $\pi/4$ DQPSK modulation for an input of data rate of $2Mbps$, which is represented by its equivalent NRZ data stream (a_k). The NRZ data stream is applied to a Serial to Parallel (S/P) converter. The output of the S/P converter (I_k, Q_k) are then applied to a differential encoder that encodes $I(t)$ and $Q(t)$ into signals $u(t)$ and $v(t)$ according to Eq.(3) and Eq.(4). The output of the differential encoder is represented by dual constellation diagram that shows the two separate constellations with identical Gray coding but rotated by 45° with respect to each other as shown in Fig.(5a) [16]. One of the main properties of the (u, v) signals represented by the constellation diagram in Fig.(5a) that it does not have any paths through the origin. Consequently, the maximum phase shift is reduced to 135° which leads to a lower dynamic range of fluctuations.

$$u_k = (u_{k-1}I_k) - (v_{k-1}Q_k) \quad (3)$$

$$v_k = (u_{k-1}I_k) + (v_{k-1}Q_k) \quad (4)$$

All physical channel mediums have limited bandwidth. Thus, utilizing Rectangular (Rect) pulse as a pulse shaping will lead to distortion in both signal amplitude and phase which is called Inter Symbol Interference (ISI). Hence, in our $\pi/4$ DQPSK model the signals $u(t)$ and $v(t)$ are applied to a Square Root Raised Cosine filter (SRRC) filter with a roll-off factor $\alpha = 0.4$, and an impulse response according to: Eq.(4). This results in a continuous phase and bandwidth-efficient modulation. On the other hand, it is much more sensitive to channel fluctuations (Envelope Fluctuation).

$$h(t) = \frac{4\propto}{\pi\sqrt{T}} \frac{\cos\left(\frac{(1+\propto)\pi t}{T}\right) + \frac{T}{4\alpha t}\sin\left(\frac{(1+\propto)\pi t}{T}\right)}{1 - \left(\frac{4\alpha t}{T}\right)^2} \quad (5)$$

Equation(6) shows the output of the π/4 DQPSK modulator without the SRRC filter.

$$S_k(t) = u_k\cos(2\pi f_c t) + v_k sin(2\pi f_c t) \quad (6)$$

The (I, Q) signals are then up-converted to the IF frequency band to convert the signals to complex envelop representation and select positive pre-envelop. The output of the $\pi/4$ DQPSK

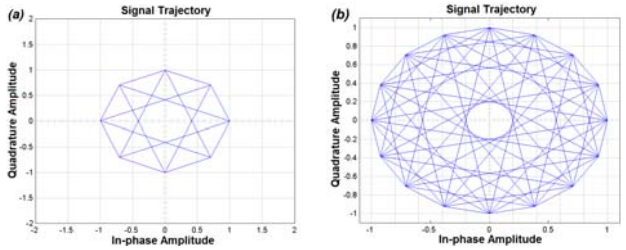

Fig. 5. Standard Signal Constellation Diagrams Generated with Matlab Simulink: (a) $\pi/4$ DQPSK, (b) $\pi/8$ D8PSK.

modulator is applied to the AFH sub system followed by the RF frequency up-conversion.

In the receiver path, after applying received phase signals (I, Q) to SRRC matched filter we use differential decoding scheme. The differential decoder calculates the sign of, $[I_k, Q_k, I_{k-1}, Q_{k-1}]$ and output the recovered sent data symbols (u, v) as shown in Fig.(6) [15], [17].

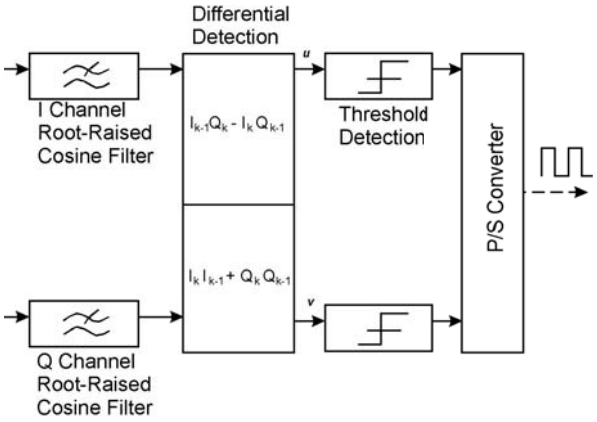

Fig. 6. $\pi/4$ DQPSK Demodulator Utilizing Differential Decoding.

C. $\pi/8$ D8PSK Modulation

In this section, we present the third modulation scheme that is utilized in our Bluetooth transceiver which is the $\pi/8$ D8PSK. The standard 8PSK is another special modulation scheme of the original PSK modulation technique. It modulates the signal such that every 3bits constitute one symbol. The standard constellation diagram is generated by shifting the phase of the symbols $45°$. The 8PSK outperforms the QPSK from the bandwidth efficiency wherein the 8PSK reaches a data rate of $3Mbps$.

In our $\pi/8$ D8PSK model we utilize the same modulation and demodulation schemes of the $\pi/4$ DQPSK. the main difference is in the baseband modulator where two separate constellations with identical Gray coding but rotated by $22.5°$ with respect to each other as shown in Fig.(5b) are used. This maintains the same advantages of the $\pi/4$ DQPSK while the $\pi/8$ rotation also stands for simpler non-coherent detection [5].

V. Experimental Results

In this section, experimental results concerning the influence of employing GFSK, $\pi/4$ DQPSK and $\pi/8$ D8PSK modulation schemes to the performance in terms of BER, spectral efficiency, and hardware complexity are presented.

First, we examine the effect of the pulse shaping filters on the time and frequency domain output signals of the transmitter including the AFH section. Figure(7) illustrates the outputs of the transmitter IF section utilizing the three modulation techniques. It clearly demonstrates the hopping sequence and the envelop fluctuations for the $\pi/4$ DQPSK and $\pi/8$ D8PSK modulation schemes versus the constant envelop for GFSK modulation scheme.
The envelop fluctuations require semi-linear power amplifier and that leads to a lower power efficiency. Since, Bluetooth devices are almost battery powered it is preferred to utilize the GFSK modulation for low data rate applications.

Figure(8) illustrates power spectrum density for each transmitting pulse shape related to the ideal pulse (Rect NRZ Pulse).
The BT and α factors are important parameters since they control the decay of the $sinc^2$ tails that affect the BER under frequency-selective fading environments. Its found that using SRRC filter with $\alpha = 0.4$ will have better decay in side-loop suppressions than Gaussian filter with $BT = 0.5$ which leads to better channel selectivity. Therefore, the $\pi/4$ DQPSK and $\pi/8$ D8PSK modulation schemes have higher bandwidth efficiency compared to the GFSK.

Second, In order to examine the the behavior of the signal constellation under various pulse shaping filters discrete scatter plots are obtained.
Since, GFSK modulation employs the Gaussian function as a pulse shaping filter, to reduce transmission bandwidth, Fig.(9a) and Fig.(9b) illustrates the discrete-time scatter and phasor (trajectory) plots of the in-phase and quadrature signals modulated with GFSK at the transmitter side.

Figure(9c) and Fig.(9d) shows the discrete-time scatter and phasor plots of the in-phase and quadrature signals at the receiver side that clearly illustrates the impact of utilizing AWGN channel.
The $\pi/4$ DQPSK and $\pi/8$ D8PSK modulation schemes employ the SRRC filter as a pulse shaping filter to reduce transmission bandwidth and avoid the ISI. Figure(10) illustrates scatter plots of the phasor of the in-phase and quadrature signals at the transmitter side.
It is obvious from Fig.(5) and Fig.(10) that the pulse shaping filters in general have some side effects on the signal trajectory transitions as it convert constellation state points to multiple points and it smooth the edges which do not allow the receiver to give exact decisions regarding the received symbols.

Finally, the performance of the simulated system, with different modulation schemes, is determined through the calculation of the BER by Monte Carlo analysis and theoretical analysis supported by Matlab in which the system BER is plotted against different bit energy to noise ratio E_b/N_0. The

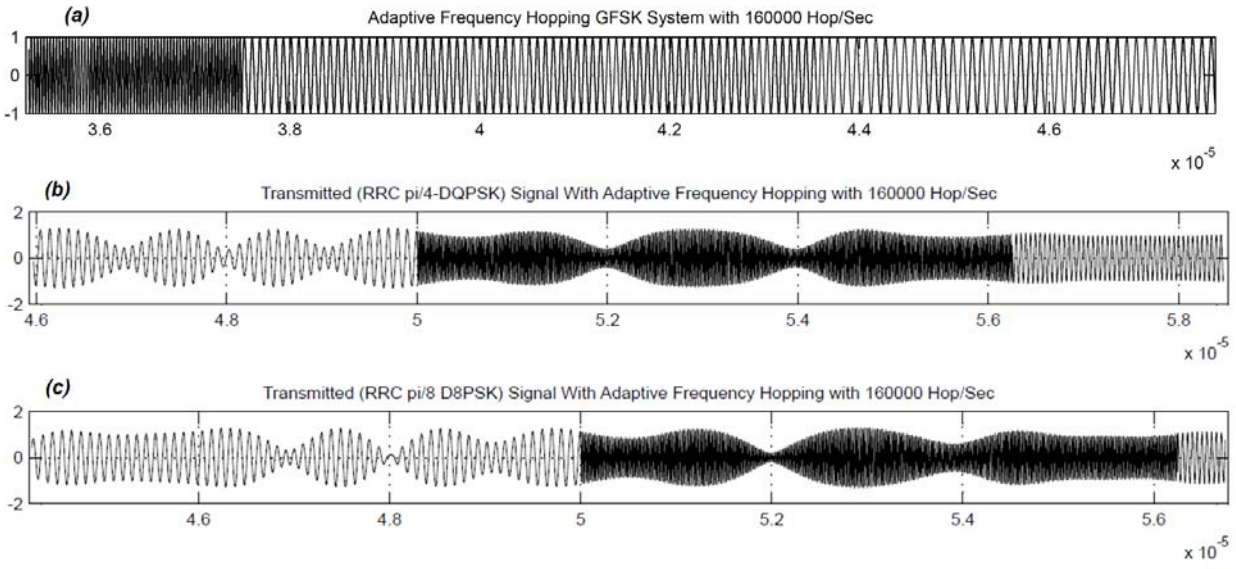

Fig. 7. Transmitter Modulated Waveforms after Applying FHSS: (a) Utilizing GFSK, (b) Utilizing $\pi/4$ DQPSK, (c) Utilizing $\pi/8$ D8PSK. - Units: Horizontal Axis Time in Seconds and Vertical Axis Amplitude.

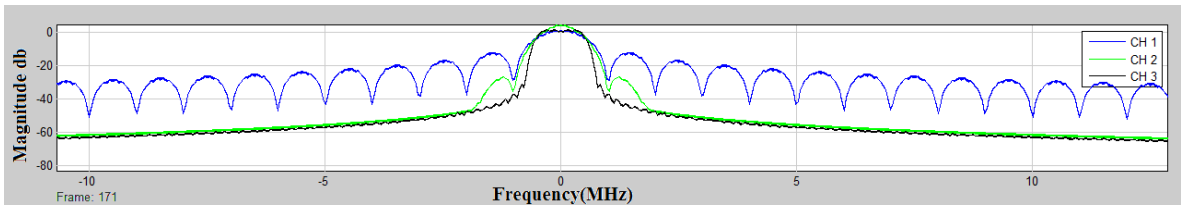

Fig. 8. Data PSD after Pulse Shaping Filter: (Ch1) NRZ Ideal Rect. Pulse Shape, (Ch2) After Utilizing Gaussian Pulse , (Ch3) After Utilizing SRRC Pulse. - Units: horizontal axis Frequency in MHz and vertical axis Power in dB.

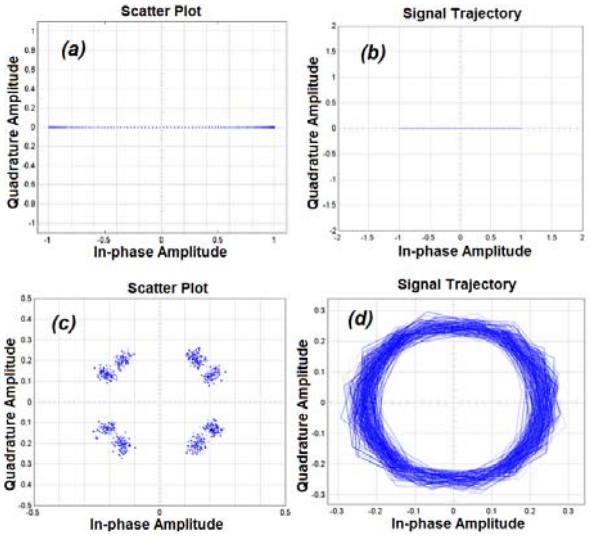

Fig. 9. Impact of Gaussian Filter on Constellation Diagram: (a) TX Scatter Plot, (b) TX Signal Trajectory, (c) RX Scatter Plot, (d) RX Signal Trajectory.

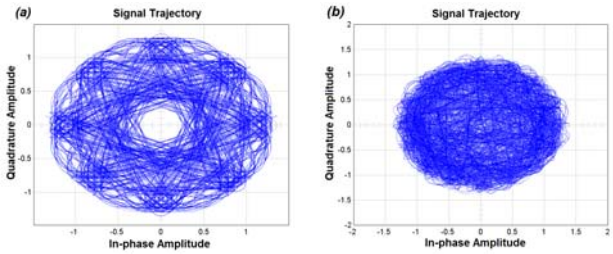

Fig. 10. Impacts of SRRC Filter in Constellation Diagram on: (a) $\pi/4$ DQPSK, (b) $\pi/8$ D8PSK.

modulation index utilized in our GFSK modulation equal 0.35 and frequency deviation of $175KHz$. All the BER calculations are performed considering the systems are utilizing AWGN channel.

In Fig.(11a) the curve representing ideal CPFSK with $\beta = 0.35$ modulation scheme BER is traced by theoretical analysis while the points representing the Bluetooth system using GFSK modulation technique with/without FHSS are calculated and traced by the Monte Carlo analysis. In the same man-

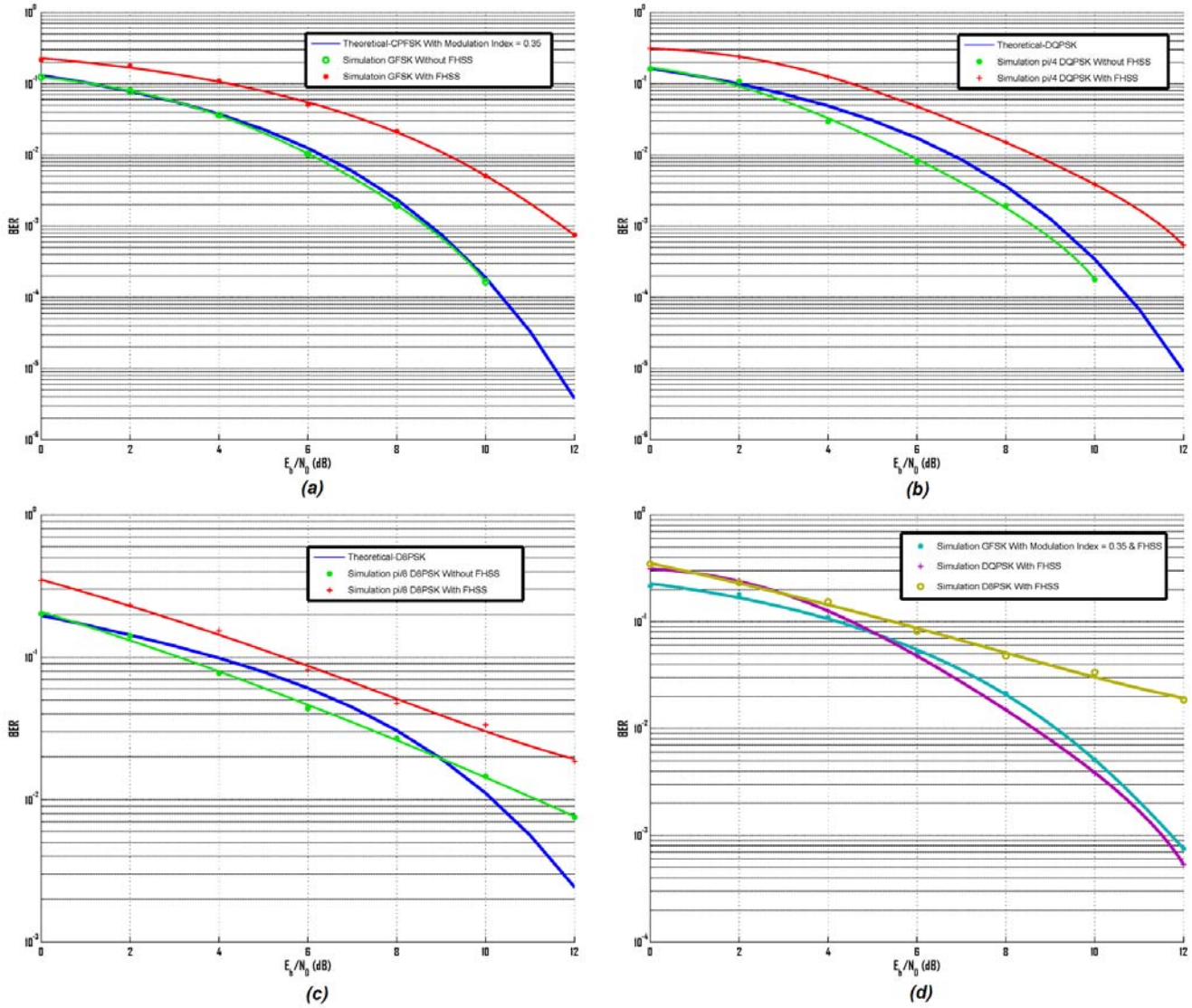

Fig. 11. BER Comparisons: (a) Between Theoretical CPFSK with $\beta = 0.35$ and Simulation Results of GFSK Systems With/Without FHSS. (b) Between Theoretical DQPSK and Simulation Results of SRRC $\pi/4$ DQPSK Models With/Without FHSS. (c) Between Theoretical D8PSK and Simulation Results of SRRC $\pi/8$ D8PSK Systems Model With/Without FHSS. (d) Between All Simulation Models With FHSS.

ner, Fig.(11b) shows a BER comparison between theoretical DQPSK modulation technique and simulation results of our system while utilizing SRRC pulse shaping filter and $\pi/4$ DQPSK modulation scheme with/without FHSS. Similarly, Fig.(11c) compares the BER between theoretical D8PSK modulation scheme and the simulation results of our system while employing $\pi/8$ D8PSK modulation method with/without FHSS.

It is clear from Fig.(11) that the BER of our simulated system utilizing GFSK, $\pi/4$ DQPSK and $\pi/8$ D8PSK without FHSS circuitry is closely tracking the theoretical CPFSK with $\beta = 0.35$, the theoretical DQPSK and the theoretical D8PSK respectively.

While the BER in case of adding FHSS circuitry to our simulated system utilizing GFSK, $\pi/4$ DQPSK and $\pi/8$ D8PSK is getting worse by $3dB$, $2.3dB$ and $3dB$ with respect to the theoretical CPFSK with $\beta = 0.35$, the theoretical DQPSK and the theoretical D8PSK respectively. These BER increase are mainly due to the minor deviation in phase and frequency of the recovered hopping sequence at the receiver end.

Figure(11d) compares the BER of the simulated system utilizing the aforementioned digital modulation techniques with FHSS with respect to each other. It is clear that the best performance is achieved by $\pi/4$ DQPSK followed by GFSK with $0.24dB$ then $\pi/8$ D8PSK gives the worst performance by $4.6dB$ form GFSK.

As we mentioned before, FHSS is the main advantage of the Bluetooth over other wireless communication systems. While the FHSS positively contribute to the performance in the Rayleigh fading channel it negatively affects the performance in the AWGN channel [18].

VI. Conclusion

In this paper, we have illustrated the evolution of the Bluetooth performance under the influence of different digital modulation schemes. Different pulse shaping waveforms are utilized in our simulated systems namely; Gaussian and SRRC filters. The scatter plots confirm the behavior of pulse shaping filters effects on the time and frequency domain output signals of the transmitter including the FHSS circuitry. It is found that utilizing SRRC filter has better decay in side-loop suppressions than Gaussian filter, which leads to better channel selectivity. Therefore, the $\pi/4$ DQPSK and $\pi/8$ D8PSK modulation schemes have higher bandwidth efficiency compared to the GFSK.

The performance of our simulated Bluetooth physical layer with AWGN channel is evaluated by means of the BER under the pre-mentioned pulse shapes. It has been proven by simulation results that $\pi/4$ DQPSK model achieves the best performance under AWGN channel. While the $\pi/8$ D8PSK attains the highest data rate. Moreover, the effect of the FHSS on the performance in terms of BER is analyzed. The work in this paper is a first step towards a SDR-based implementation of the Bluetooth transceiver using Universal Software Radio Peripheral (USRP) $N210$ platform.

References

[1] T. Svedek, M. Herceg, and T. Matic, "A Simple Signal Shaper for GMSK/GFSK and MSK Modulator Based on Sigma-Delta Look-up Table," *Journal of Radio Engineering*, vol. 18, no. 2, pp. 230–237, June 2009.

[2] J. Gillen, "Modulation techniques in bluetooth wireless technology," *ECE440 White Paper*, November 2002.

[3] *Bluetooth 802.15.1: Specification of the Bluetooth System*, ver. 1.2 ed., IEEE, August 2003. [Online]. Available: http://standards.ieee.org

[4] *Specification of the Bluetooth EDR System: Covered Core Package*, ver. 2.0 ed., Bluetooth Organization, November 2004. [Online]. Available: www.Bluetooth.org

[5] Y. Choi, H. B. Lee, S.-B. Park, B.-H. Hong, S.-Y. Lee, and K. H. Tchah, "A unified gfsk, p/4-shifted dqpsk, and 8-dpsk baseband controller for enhanced data rate bluetooth soc," *Current Applied Physics*, vol. 6, no. 5, pp. 862 – 872, 2006.

[6] K. Shuaib, M. Alnuaimi, M. Boulmalf, I. Jawhar, F. Sallabi, and A. Lakas, "Performance Evaluation of IEEE 802.15.4: Experimental and Simulation Results," *Journal of Communications JCM*, vol. 2, no. 4, pp. 29–37, June 2007.

[7] D. Spill and A. Bittau, "Bluesniff: Eve meets alice and bluetooth," in *Proceedings of the first USENIX workshop on Offensive Technologies*, ser. WOOT'07. Berkeley, CA, USA: USENIX Association, 2007, pp. 5.1–5.10.

[8] L. Binh and T. Huynh, "Linear and nonlinear distortion effects in direct detection 40gb/s msk modulation formats multi-span optically amplified transmission," *Optics Communications*, vol. 273, no. 2, pp. 352 – 361, 2007.

[9] R. Kanna, "Design of ZigBee Transceiver for IEEE 802.15.4 Using MATLAB/SIMULINK," Master of Technology Disseration, National Institute of technology, ROURKELA, ODISHA, INDIA, 2011.

[10] K. Morsi, X. Huagang, and G. Qiang, "Performance estimation and evaluation of bluetooth frequency hopping selection kernel," in *Joint Conferences on Pervasive Computing*, ser. JCPC'09, dec. 2009, pp. 461 –466.

[11] R. Schiphorst, F. Hoeksema, and K. Slump, "Bluetooth demodulation algorithms and their performance," in *nd Karlsruhe Workshop on Software Radios*, 2002, pp. 99–106.

[12] *Bluetooth 802.15.1: Specification of the Bluetooth System*, ver. 1.1 ed., IEEE, June 2002. [Online]. Available: http://standards.ieee.org

[13] *Bluetooth 802.15.2 IEEE Standard: Coexistence of Wireless Personal Area Networks with Other Wireless Devices Operating in Unlicensed Frequency Bands*, IEEE, 2003. [Online]. Available: http://standards.ieee.org

[14] M. Simon, *Bandwidth-Efficient Digital Modulation With Application to Deep-Space Communications*, ser. Deep-Space Communications and Navigation Series. Wiley-Interscience, 2003.

[15] D.-C. Chang, "Least Squares/Maximum Likelihood Methods for the Decision-Aided GFSK Receiver," *IEEE Signal Processing Letters*, vol. 16, pp. 517–520, 2009.

[16] F. Xiong, *Digital Modulation Techniques, Second Edition (Artech House Telecommunications Library)*. Norwood, MA, USA: Artech House, Inc., 2006.

[17] K. Gentile, "The care and feeding of digital pulse shaping filters," *www.rfdesign.com*, pp. 50 – 61, 2002.

[18] K. Du and N. Swamy, *Wireless Communication Systems: From RF Subsystems to 4G Enabling Technologies*. Cambridge University Press, 2010.